



Contents lists available at ScienceDirect

Biochemical and Biophysical Research Communications

journal homepage: [www.elsevier.com/locate/ybbrc](http://www.elsevier.com/locate/ybbrc)

# Synchronous spike patterns in differently mixed cultures of human iPSC-derived glutamatergic and GABAergic neurons

Takuya Sasaki <sup>a, b, \*\*</sup>, Ikuro Suzuki <sup>c, d, e, \*</sup>, Remi Yokoi <sup>c</sup>, Kaoru Sato <sup>d, e, f</sup>, Yuji Ikegaya <sup>a, g</sup>

<sup>a</sup> Graduate School of Pharmaceutical Sciences, The University of Tokyo, 7-3-1 Hongo Bunkyo-ku, Tokyo, 113-0033, Japan

<sup>b</sup> Precursory Research for Embryonic Science and Technology, Japan Science and Technology Agency, 4-1-8 Honcho, Kawaguchi, Saitama, 332-0012, Japan

<sup>c</sup> Department of Electronics, Graduate School of Engineering, Tohoku Institute of Technology, 35-1 Yagiyama Kasumicho, Taihaku-ku, Sendai, Miyagi, 982-8577, Japan

<sup>d</sup> iPS-non-Clinical Experiments for Nervous System (iNCENS) Project, Kanagawa, Japan

<sup>e</sup> Consortium for Safety Assessment using Human iPS Cells (CSAHi), Kanagawa, Japan

<sup>f</sup> Laboratory of Neuropharmacology, Division of Pharmacology, Laboratory of Neuropharmacology, National Institute of Health Sciences, Tokyo, Japan

<sup>g</sup> Center for Information and Neural Networks, Suita City, Osaka, 565-0871, Japan

## ARTICLE INFO

### Article history:

Received 5 March 2019

Accepted 24 March 2019

Available online 4 April 2019

### Keywords:

Human induced-pluripotent stem cell-derived neurons  
Cell type  
Synchronization  
Multielectrode array

## ABSTRACT

Human induced-pluripotent stem cell (hiPSC)-derived neurons develop organized neuronal networks under in vitro cultivation conditions. Here, using a multielectrode array system, we examined whether the spike patterns of hiPSC-derived neuronal populations differed in a manner that depended on the proportions of glutamatergic and gamma-aminobutyric acid (GABA)ergic neurons in the cultures. Synchronous burst firing events spanning multiple electrodes became more frequent as the number of days in culture increased. However, at all developmental stages, the event rates of synchronous burst firing, the repertoires of synchronous burst firing, and the frequencies of sporadic spikes did not differ in cultures with different glutamatergic-to-GABAergic ratios. Pharmacological blockade of GABAergic synaptic transmission increased the frequencies of spike patterns specifically in cultures with lower glutamatergic-to-GABAergic ratios. These results demonstrate that a robust homeostatic property of developing hiPSC-derived neuronal networks in culture counteracts chronically imbalanced glutamatergic and GABAergic signaling.

© 2019 Elsevier Inc. All rights reserved.

## 1. Introduction

Cultures of human induced-pluripotent stem cell (hiPSC)-derived neurons have been utilized as useful in vitro model systems that are expected to replicate human neuronal networks more accurately than rodent neurons and that can be used in disease modeling and drug discovery research [1–4]. During the maturation of dissociated hiPSC-derived neurons in culture, the cells establish intricate neuronal networks by forming synaptic

connections [2,5–7] and begin to display organized spatiotemporal activity patterns [2,8–10], a physiological sign that suggests successful incorporation of individual neurons into functional circuits.

The mammalian cortex is mainly composed of excitatory glutamatergic (Glu) and inhibitory gamma-aminobutyric acid (GABA)ergic neurons; the ratio of glutamatergic neurons to GABAergic neurons is approximately 80:20 throughout rodent cortical regions [11,12]. The relative numbers of these cell types are crucial for achieving appropriate net excitatory and inhibitory balances to stabilize neuronal activity levels.

The evidence raises the question of whether and how activity patterns of neuronal populations differ depending on the existence ratios of glutamatergic and GABAergic cell types. To address this question, hiPSC-derived neuron cultures are an ideal experimental system as we can artificially manipulate the proportions of cell types of hiPSC-derived neurons [13–15]. Here, we cocultured hiPSC-derived glutamatergic and GABAergic neurons at various ratios (Fig. 1A). The spike patterns of these hiPSC-derived neuronal

**Abbreviations:** hiPSC, human induced-pluripotent stem cell; GABA, gamma-aminobutyric acid; Glu, glutamate; SBF, synchronous burst firing; PTX, picrotoxin.

\* Corresponding author. Department of Electronics, Graduate School of Engineering, Tohoku Institute of Technology, 35-1 Yagiyama Kasumicho, Taihaku-ku, Sendai, Miyagi, 982-8577, Japan.

\*\* Corresponding author. Graduate School of Pharmaceutical Sciences, The University of Tokyo, 7-3-1 Hongo Bunkyo-ku, Tokyo, 113-0033, Japan.

E-mail addresses: [tsasaki@mol.f.u-tokyo.ac.jp](mailto:tsasaki@mol.f.u-tokyo.ac.jp) (T. Sasaki), [i-suzuki@tohtech.ac.jp](mailto:i-suzuki@tohtech.ac.jp) (I. Suzuki).

<https://doi.org/10.1016/j.bbrc.2019.03.161>

0006-291X/© 2019 Elsevier Inc. All rights reserved.

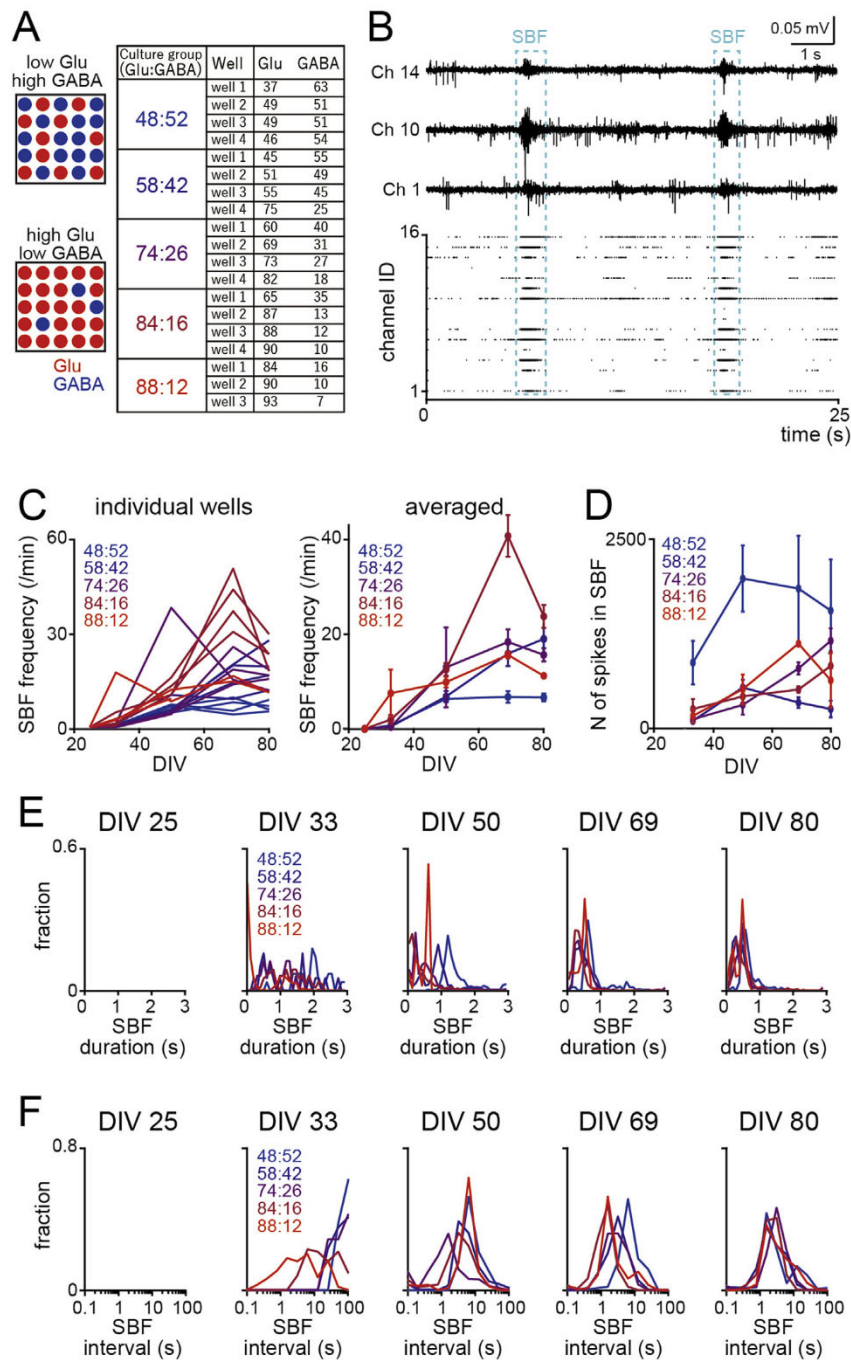


**Fig. 1. Synchronized burst activity of hiPSC-derived glutamatergic and GABAergic neurons.** (A) (Left) Schematic illustrations of cocultures of hiPSC-derived glutamatergic (red) and GABAergic (blue) neurons. The ratios of glutamatergic (red) and GABAergic (blue) neurons in individual wells analyzed in this study are summarized in the table at right. (B) (Top) Representative electrophysiological traces from three channels, including two typical synchronous burst-like population firing (SBF) events (indicated by the cyan boxes). In addition, each channel recorded sporadic spikes outside the SBF events. (Bottom) Raster plot showing spike patterns detected in all 16 electrodes. Each row represents an electrode, and each tick represents a spike. (C) (Left) Data from individual wells. Developmental changes in the frequency of SBF events occur as DIV increases. Each line indicates a well. (Right) Averaged data computed from each culture group. The data are presented as the mean  $\pm$  standard error of the mean (SEM). (D) Total number of spikes recorded by active electrodes included in a single SBF event. The data are presented as the mean  $\pm$  SEM. (E) Distribution of the duration of SBF events at each DIV. (F) Distribution of the intervals between neighboring SBF events at each DIV.

populations were monitored using a multielectrode array (MEA) system as previously reported [2,9,10,16]. We focused our analyses on the synchronous burst firing patterns and sporadic spike patterns of the hiPSC-derived neurons during progressive developmental stages. We then tested the effects of inhibition of GABAergic transmission on the temporal activity patterns of the hiPSC-derived neuronal cultures.

## 2. Material and methods

### 2.1. Culture of hiPSC-derived neuronal networks at varying ratios of glutamatergic neurons to GABAergic neurons

Human iPSC-derived layer V glutamatergic neurons (BX-0350; BrainXell Inc.) and PV-enriched GABAergic neurons (BX-0451;

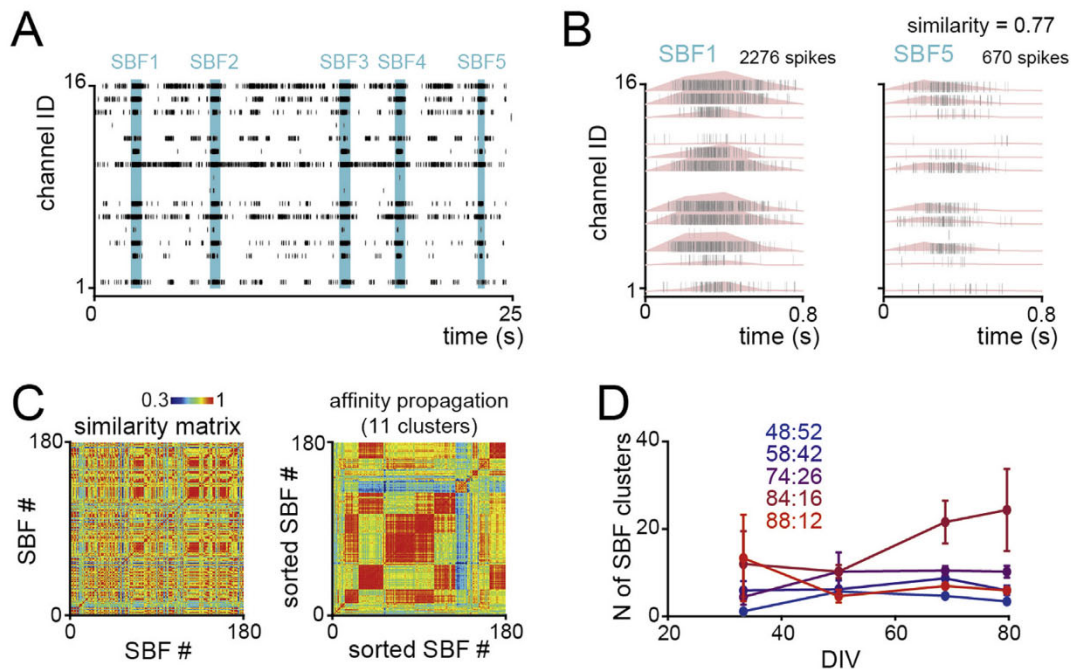


**Fig. 2.** Variability of SBF events depends on the ratio of glutamatergic to GABAergic cells. (A) Raster plot including five SBF events. (B) Two representative SBF events (SBF 1 and SBF 5) shown in A are magnified. Each tick shows a spike, and the corresponding spike rate changes recorded by individual channels are superimposed in pink. The similarity of the two SBF events was calculated to be 0.77. (C) (Left) Similarity matrix of all SBF event pairs constructed from the raster plot in A. (Right) The left matrix was clustered using the affinity propagation algorithm, which identified 11 SBF clusters. (D) Number of SBF clusters as a function of DIV. The data are presented as the mean  $\pm$  SEM.

BrainXell Inc.) were seeded in 24-well MEA plates (Comfort, Eco, Alpha Med Scientific Inc.) coated with polyethyleneimine (Sigma) and Laminin-511 (Nippi) at ratios of 100/0, 75/25, 50/50, 25/75, and 0/100 (glutamatergic neurons:GABAergic neurons). The cell density at all ratios was  $8.0 \times 10^5$  cells/cm<sup>2</sup>. A seeding medium was used to seed the cells; on the following day, the medium was changed to Day 1 Medium, and the medium was changed again after 4 days to Day 4 Medium. Half of the culture medium was replaced with fresh Day 4 Medium on days 7, 11, and 14. On day 8,  $3 \times 10^4$  astrocytes (AX0084; Axol Bioscience Inc.) were added to each well. BrainPhys medium containing SM 1 neuronal supplement (STEMCELL Technologies) was used after day 18 and was replaced every 4 days.

## 2.2. MEA measurements

Spontaneous extracellular field potentials were acquired using a 24-well MEA system (Presto; Alpha Med Scientific Inc.) at a 20 kHz/channel sampling rate at 37 °C under 5% CO<sub>2</sub>. Signals were high-pass-filtered at 1 Hz and stored on a personal computer. Spikes were detected in the acquired data using a 100-Hz high-pass filter.

## 2.3. Pharmacological tests

To evaluate the function of glutamate receptors at each cell type ratio, 10  $\mu$ M picrotoxin was added in the 8th week of culture. The spontaneous activity in the presence of each drug at each concentration was measured for 10 min.

## 2.4. Detection of spikes

Spikes were detected using Mobius software (Alpha Med Scientific Inc.). A spike was counted when the extracellularly recorded signal exceeded a threshold of  $\pm 5.3 \sigma$ , where  $\sigma$  represents the standard deviation of the baseline noise during quiescent periods.

SBFs were detected via MED64 spikes analysis (Alpha Med Scientific Inc.).

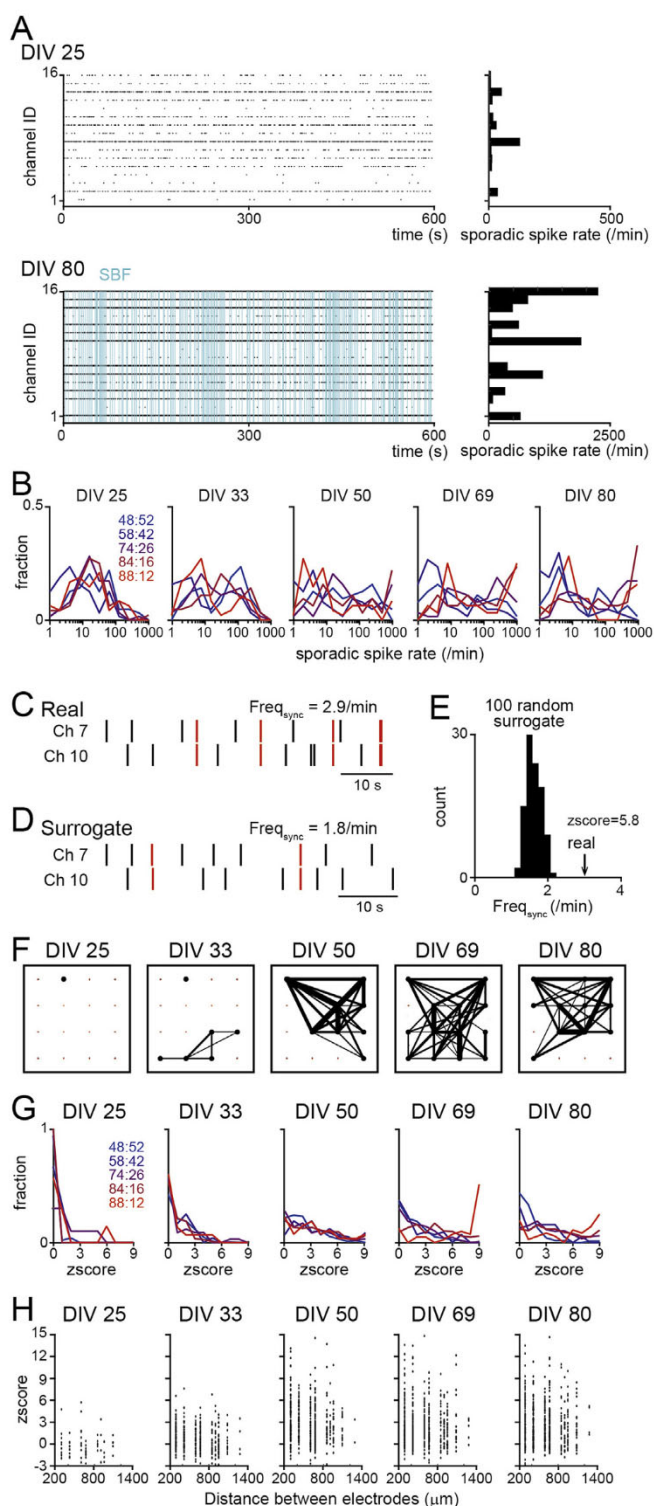
## 2.5. Statistics

Electrodes that recorded spike rates of more than 1 Hz were defined as active electrodes. To obtain the data shown in Figs. 2B, 3D, active electrodes were analyzed. Comparisons of two sample distributions were performed using the Kolmogorov-Smirnov test. Multiple group comparisons were performed using post hoc Bonferroni correction. In Fig. 4A, because the number of samples was relatively low ( $n = 3-4$ ), a statistical  $P$ -value was computed by applying a permutation test of within-group averaged data. The null hypothesis was rejected at the  $P < 0.05$  level.

## 3. Results

### 3.1. Synchronous burst firing events of hiPSC-derived neurons

Human iPSC-derived neurons were plated on MEA-containing culture dishes equipped with 16 recording electrodes as described previously [2,9,10,16]. In this study, hiPSC-derived neurons were initially seeded at varying ratios of glutamatergic to GABAergic cells (100:0, 75:25, 50:50, 25:75, and 0:100); this resulted in culture preparations with different existence ratios of glutamatergic and GABAergic cells (88:12, 84:16, 74:26, 58:42, and 48:52), respectively, as shown by immunocytochemistry using an antibody against  $\beta$ -tubulin III, a neuronal marker, and an antibody against GABA, a marker of GABAergic neurons (Fig. 1A; for more detail, see Yokoi et al., submitted for publication). Electrophysiological recordings were obtained at 25, 33, 50, 69, and 80 days in vitro (DIV). The cultures spontaneously exhibited synchronous burst firing (SBF) events spanning multiple electrodes (Fig. 1B). As shown in the lower raster plot, which represents the spontaneous



Sasaki et al., Figure 3

**Fig. 3. Characteristics of sporadic spikes produced by hiPSC-derived neurons.** (A) (Left) Rastergrams showing the spiking activity patterns detected by 16 electrodes at DIV 25 and DIV 80. Each row represents a single electrode, and each dot represents a single spike. The spikes involved in SBF events appear in the cyan regions. (Right) Sporadic spike frequencies of the individual electrodes corresponding to the left raster plot. (B) Distribution of sporadic spike rates in each culture group at each DIV. (C) (Left) Spike patterns recorded by two representative electrodes (top). Each vertical line represents a spike. The number of synchronized spikes ( $\text{Freq}_{\text{sync}}$ ) within a 100-ms time window was counted. (D) A typical surrogate dataset was generated by randomly

spiking patterns of individual channels, ongoing spike rates were markedly increased during SBF events.

The frequency of SBF events at each DIV is summarized in Fig. 1C. In all culture groups, the frequency of SBF events was zero on DIV 25 and significantly increased with time up to DIV 80 (88:12,  $F(4,8) = 4.23$ ,  $P = 0.039$ ; 84:16,  $F(4,14) = 45.19$ ,  $P = 7.4 \times 10^{-8}$ ; 74:26,  $F(4,15) = 4.66$ ,  $P = 0.012$ ; 58:42,  $F(4,15) = 19.45$ ,  $P = 8.4 \times 10^{-6}$ ; 48:52,  $F(4,15) = 21.17$ ,  $P = 2.8 \times 10^{-6}$ ; one-way ANOVA). At all DIVs, the mean SBF event frequencies in cultures of the 88:12 group were significantly higher than those in cultures of the 48:52 group (88:12 vs. 48:52:  $F(1,16) = 35.30$ ,  $P = 0.004$ , repeated-measure ANOVA with Bonferroni corrections), demonstrating that iPSC-derived neuronal populations with higher proportions of glutamatergic cells were more likely to produce SBF events. However, no significant differences in the frequencies of SBF events were detected in any other group comparisons ( $P > 0.05$ ). Repeated-measures ANOVA with Bonferroni correction revealed no significant difference in the number of spikes included in a single SBF event across culture groups ( $P > 0.05$ ). The distributions of the durations and inter-event intervals of the SBF events are summarized in Fig. 1E and F.

Using correlation analysis, we then examined temporal spike patterns within SBF events. Fig. 2A shows representative spike patterns and SBF events. In the raster plots in Fig. 2B, the first (SBF 1) and the fifth (SBF 5) SBF events are magnified on the time axis. For every 0.2-s bin within a SBF event, instantaneous spike rates were computed for individual electrodes, and a series of population vectors representing a SBF-associated spiking pattern was constructed. The Pearson correlation coefficient between each pair of population vectors was computed based on the similarity of spike patterns. The same analysis was applied to all possible pairs of SBF events, creating a similarity matrix for all SBF events that occurred during a 10-min recording period (Fig. 2C, left). The matrix was then analyzed using the affinity propagation algorithm, an exemplar-based method of clustering analysis, to identify clusters of SBF events, including similar spiking patterns. In the sample data shown in Fig. 2C, the affinity propagation identified 11 clusters. The numbers of clusters of SBF events detected in all the recordings are summarized in Fig. 2D. Throughout the culture period, the number of clusters at a given DIV did not differ in any of the culture groups (in all comparisons,  $P > 0.05$ , repeated-measures ANOVA with Bonferroni correction). The results demonstrate that the hiPSC-derived neuronal populations generated almost identical repertoires of SBF-associated spiking patterns irrespective of the ratio of glutamatergic to GABAergic cells in the neuronal cultures.

### 3.2. Sporadic spike patterns of hiPSC-derived neurons

We next examined whether the spike patterns of hiPSC-derived neurons that occurred outside SBF event periods, termed sporadic spikes, differed as a function of Glu/GABA ratio and/or DIV. Fig. 3A shows representative sporadic spike patterns observed outside SBF events (vertical cyan lines). On any DIV, the distributions of

transposing the inter-spike intervals (ISIs) within an electrode. (E) For this electrode pair, a real  $\text{Freq}_{\text{sync}}$  value is indicated by the arrow; this value was compared with the  $\text{Freq}_{\text{sync}}$  distribution computed from the corresponding 100 surrogate datasets (histogram). Based on the distribution of the surrogate datasets, the z-score of the real data was calculated to be 5.8. (F) Representative map showing highly correlated electrode pairs; pairs with z-scores greater than 1.96 are connected by black lines. The thickness of the line indicates the z-score. The large black dots and small red dots represent active and non-active electrodes, respectively. (G) Distribution of z-scores for each pair of active electrodes. (H) Plot of z-scores for individual active electrode pairs against the distance between the two electrodes. Black dots show individual electrode pairs; red dots show averaged data.

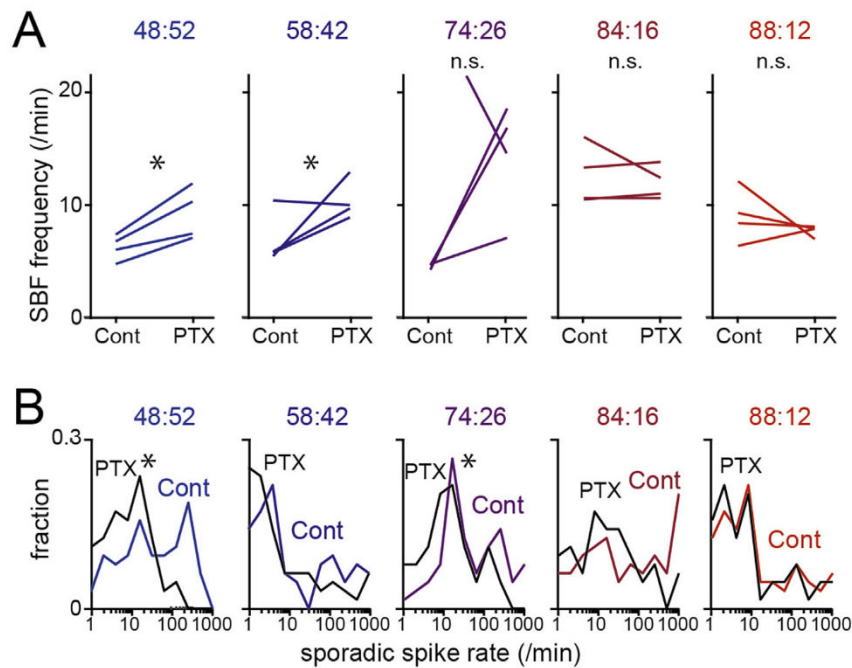


**Fig. 4.** Inhibition of GABAergic transmission alters spiking activity. (A) Changes in the frequency of SBF events during application of PTX. Asterisks denote permutation  $P$ -values of less than 0.05. (B) Distribution of the sporadic spike rates recorded by individual electrodes. The black lines indicate data obtained in the presence of PTX. Asterisks denote  $P < 0.05$  between control and PTX data according to the Kolmogorov-Smirnov test.

sporadic spike rates did not differ across groups with different Glu/GABA ratios (Fig. 3B; all DIVs:  $P > 0.05$ ; Kolmogorov-Smirnov test with Bonferroni correction). These results demonstrate that hiPSC-derived neurons showed increased sporadic spiking as DIV increased but that the activity pattern at each developmental stage did not depend on the relative proportions of glutamatergic and GABAergic cells. However, while statistical significance was not found, it is notable that a small proportion (10–20%) of electrodes in the high Glu/GABA cultures (88:12, 84:16, and 74:26) recorded extremely high spike rates of more than 500/min after DIV 50.

To further investigate the temporal correlations of sporadic spikes, we next applied pairwise synchronization analysis. In a pair of electrodes, coincident sporadic spikes recorded within a 100-ms period were extracted as synchronous sporadic spikes. The frequency of such synchronous sporadic spikes ( $\text{Freq}_{\text{sync}}$ ) was computed (Fig. 3C). Surrogate  $\text{Freq}_{\text{sync}}$  datasets were obtained using Monte-Carlo randomization in which inter-sporadic spike intervals (ISIs) were shuffled within each electrode to collapse the temporally organized spike patterns without changing the total spike counts (Fig. 3D). This shuffling procedure was repeated 100 times, and the probability distribution of  $\text{Freq}_{\text{sync}}$  in the surrogate datasets was compared with the real  $\text{Freq}_{\text{sync}}$  (Fig. 3E). In the sample electrode pair, the real  $\text{Freq}_{\text{sync}}$  was  $2.9 \text{ min}^{-1}$ , whereas such a high frequency was never observed in the 100 surrogates. The significance of the real  $\text{Freq}_{\text{sync}}$  was quantified by computing a z-score based on the mean and standard deviation of the distribution of the 100 surrogate  $\text{Freq}_{\text{sync}}$ s. Fig. 3F presents representative spatial maps showing highly correlative electrode pairs with z-scores of more than 1.96 (a significance level of  $P < 0.05$ ) at various DIVs in a single well. In each culture group, the distributions of z-scores increased significantly as DIV increased up to 80 (88:12,  $F(4,121) = 12.98$ ,  $P = 7.9 \times 10^{-9}$ ; 84:16,  $F(4,649) = 35.62$ ,  $P = 6.4 \times 10^{-27}$ ; 74:26,  $F(4,511) = 13.58$ ,  $P = 1.6 \times 10^{-10}$ ; 58:42,  $F(4,142) = 8.39$ ,  $P = 4.2 \times 10^{-6}$ ; 48:52,  $F(4,731) = 29.17$ ,  $P = 1.6 \times 10^{-22}$ ; one-way ANOVA). On each DIV, the overall distribution of z-scores did not differ significantly across the culture groups (Fig. 3G; all DIVs:  $P > 0.05$ ; Kolmogorov-Smirnov test with Bonferroni correction).

These results suggest that hiPSC-derived neurons developed stronger correlative sporadic spike patterns as DIVs increased but that the correlative activity patterns observed at each developmental stage did not differ in cultures containing different ratios of glutamatergic to GABAergic cells. All z-scores were plotted as a function of the distance between the two electrodes (Fig. 3H); the results showed a significant negative correlation between z-score and distance on DIVs 33 and 50 (DIV 25,  $R = -0.031$ ,  $P = 0.80$ ; DIV 33,  $R = -0.15$ ,  $P = 0.0063$ ; DIV 50,  $R = -0.12$ ,  $P = 0.015$ ; DIV 69,  $R = -0.081$ ,  $P = 0.071$ ; DIV 80,  $R = -0.063$ ,  $P = 0.16$ ), suggesting that the synchronicity of sporadic spikes between two electrodes was associated with their interelectrode distance.

### 3.3. Inhibition of GABAergic transmission increases SBF events

We sought to examine the intrinsic contribution of GABAergic synaptic transmission to the observed neuronal activity patterns. We tested this idea by applying picrotoxin (PTX), a GABA<sub>A</sub> receptor inhibitor, to cultures on DIV 50. In the 58:42 and 48:52 groups, treatment with PTX significantly increased the frequency of SBF events (Fig. 4A; 58:42, permutation  $P$ -value for average = 0.025; 48:52, permutation  $P$ -value for average = 0.035). The other culture groups did not show significant differences ( $P > 0.05$ ). In the 74:26 and 48:52 groups, treatment with PTX also increased the frequency of sporadic spikes (Fig. 4B; 74:26,  $D_{\text{max}} = 0.31$ ,  $P = 0.0028$ ; 48:52,  $D_{\text{max}} = 0.38$ ,  $P = 1.6 \times 10^{-4}$ ; Kolmogorov-Smirnov test), whereas no significant differences were observed in the other culture groups ( $P > 0.05$ ). These results suggest that iPSC-derived neuronal cultures with lower ratios of glutamatergic to GABAergic cells were more sensitive to blockade of GABAergic signaling.

## 4. Discussion

In this study, we analyzed the spatiotemporal spike patterns exhibited by hiPSC-derived neuronal populations consisting of various proportions of glutamatergic and GABAergic cells by focusing on two activity patterns, transient excitation of neuronal

populations (SBF events) and basal activity patterns of individual neurons (sporadic spikes). These two activity patterns reflect different physiological aspects of neuronal network activity. Our major findings were as follows: (1) SBF events occurred more frequently at higher DIVs irrespective of the Glu/GABA ratios; (2) sporadic spike patterns did not vary markedly among cultures with different Glu/GABA ratios, and (3) inhibition of GABAergic transmission increased the frequency of both SBF events and sporadic spiking of hiPSC-derived neurons specifically in cultures with lower Glu/GABA ratios.

In the cortex, the majority (70–80%) of neurons are glutamatergic excitatory neurons, and the remaining neurons are GABAergic inhibitory neurons [11,12]. The balance between glutamatergic excitatory transmission and GABAergic inhibitory transmission may determine the synchronous spiking patterns of neuronal networks. In some of our experiments, the Glu/GABA ratios used might be anatomically unrealistic, but the results obtained under these conditions verify the hypothesis that the Glu/GABA ratio affects the population spike patterns. Contrary to our expectation, almost no significant difference in the frequencies of SBF events or sporadic spikes was observed in the different culture groups. These results indicate that hiPSC-derived neurons in culture have the ability to converge their activity to a certain level irrespective of the proportions of glutamatergic and GABAergic neurons in the cultures. The results also suggest that a strong homeostasis that prevents excitatory and inhibitory imbalance is inherent in hiPSC-derived neuronal networks. The mechanisms underlying the homeostatic property of these networks may include scaling of synaptic strength, adjustment of the probability of synaptic connection between pairs of neurons, adjustment of the intrinsic activity levels of individual cells, and loss of active/inactive cells. Further studies are required to elucidate the detailed biological mechanisms involved.

Cultures with lower ratios of glutamatergic to GABAergic cells (i.e., 48:52, 58:42, and 74:26) specifically showed significant increases in both synchronous and sporadic activity during pharmacological inhibition of GABAergic signaling. This result suggests that the activity of these cultured neurons in the baseline state is reduced by GABAergic transmission to the same level exhibited by cultures with higher ratios of glutamatergic to GABAergic cells. The differences in the dependence of hiPSC-derived neuronal spike activity on GABAergic signaling may emerge during the development of the neuronal networks in the cultures.

In conclusion, we demonstrated the robustness of developing hiPSC-derived neuronal networks under diverse excitatory conditions. Culture systems consisting of hiPSC-derived neurons have been widely used as models to replicate human brain networks and in drug discovery screening and toxicity testing [1,2]. One of the most critical factors in this applied research is minimization of the variability of activity patterns across different samples. In this sense, our results demonstrate that differences in the ratio of glutamatergic to GABAergic cells in such cultures do not strongly affect inter-sample variability in hiPSC-derived neuronal cultures. Further studies are needed to determine whether other types of hiPSC-derived neurons such as dopaminergic cells [17,18] display similar homeostatic properties during development in culture systems.

## Acknowledgments

This work was supported by Kaken-hi (17H05939; 17H05551) to

T.S., Kaken-hi (17K20111) to I.S., and AMED under Grant Number JP18bk0104076 (iNCENS: iPS-nonclinical experiments for nervous system) to I.S., K.S. and Y.I.

## Transparency document

Transparency document related to this article can be found online at <https://doi.org/10.1016/j.bbrc.2019.03.161>.

## References

- [1] S.J. Engle, D. Puppala, Integrating human pluripotent stem cells into drug development, *Cell Stem Cell* 12 (2013) 669–677.
- [2] A. Odawara, Y. Saitoh, A.H. Alhebshi, M. Gotoh, I. Suzuki, Long-term electrophysiological activity and pharmacological response of a human induced pluripotent stem cell-derived neuron and astrocyte co-culture, *Biochem. Biophys. Res. Commun.* 443 (2014) 1176–1181.
- [3] K. Takahashi, K. Tanabe, M. Ohnuki, M. Narita, T. Ichisaka, K. Tomoda, S. Yamanaka, Induction of pluripotent stem cells from adult human fibroblasts by defined factors, *Cell* 131 (2007) 861–872.
- [4] A.B. Cherry, G.Q. Daley, Reprogrammed cells for disease modeling and regenerative medicine, *Annu. Rev. Med.* 64 (2013) 277–290.
- [5] Y. Shi, P. Kirwan, J. Smith, H.P. Robinson, F.J. Livesey, Human cerebral cortex development from pluripotent stem cells to functional excitatory synapses, *Nat. Neurosci.* 15 (2012) 477–486, S471.
- [6] J.E. Kim, M.L. O'Sullivan, C.A. Sanchez, M. Hwang, M.A. Israel, K. Brennand, T.J. Deerinck, L.S. Goldstein, F.H. Gage, M.H. Ellisman, A. Ghosh, Investigating synapse formation and function using human pluripotent stem cell-derived neurons, *Proc. Natl. Acad. Sci. U. S. A.* 108 (2011) 3005–3010.
- [7] T. Hiragi, M. Andoh, T. Araki, T. Shirakawa, T. Ono, R. Koyama, Y. Ikegaya, Differentiation of human induced pluripotent stem cell (hiPSC)-derived neurons in mouse hippocampal slice cultures, *Front. Cell. Neurosci.* 11 (2017) 143.
- [8] K. Fukushima, Y. Miura, K. Sawada, K. Yamazaki, M. Ito, Establishment of a human neuronal network assessment system by using a human neuron/astrocyte co-culture derived from fetal neural stem/progenitor cells, *J. Biomol. Screen* 21 (2016) 54–64.
- [9] A. Odawara, H. Katoh, N. Matsuda, I. Suzuki, Physiological maturation and drug responses of human induced pluripotent stem cell-derived cortical neuronal networks in long-term culture, *Sci. Rep.* 6 (2016) 26181.
- [10] T. Kayama, I. Suzuki, A. Odawara, T. Sasaki, Y. Ikegaya, Temporally coordinated spiking activity of human induced pluripotent stem cell-derived neurons cocultured with astrocytes, *Biochem. Biophys. Res. Commun.* 495 (2018) 1028–1033.
- [11] H. Markram, M. Toledo-Rodriguez, Y. Wang, A. Gupta, G. Silberberg, C. Wu, Interneurons of the neocortical inhibitory system, *Nat. Rev. Neurosci.* 5 (2004) 793–807.
- [12] J. DeFelipe, I. Farinas, The pyramidal neuron of the cerebral cortex: morphological and chemical characteristics of the synaptic inputs, *Prog. Neurobiol.* 39 (1992) 563–607.
- [13] C.R. Nicholas, J. Chen, Y. Tang, D.G. Southwell, N. Chalmers, D. Vogt, C.M. Arnold, Y.J. Chen, E.G. Stanley, A.G. Elefanti, Y. Sasai, A. Alvarez-Buylla, J.L. Rubenstein, A.R. Kriegstein, Functional maturation of hPSC-derived forebrain interneurons requires an extended timeline and mimics human neural development, *Cell Stem Cell* 12 (2013) 573–586.
- [14] R.K. Tsunemoto, K.T. Eade, J.W. Blanchard, K.K. Baldwin, Forward engineering neuronal diversity using direct reprogramming, *EMBO J.* 34 (2015) 1445–1455.
- [15] A.X. Sun, Q. Yuan, S. Tan, Y. Xiao, D. Wang, A.T. Khoo, L. Sani, H.D. Tran, P. Kim, Y.S. Chiew, K.J. Lee, Y.C. Yen, H.H. Ng, B. Lim, H.S. Je, Direct induction and functional maturation of forebrain GABAergic neurons from human pluripotent stem cells, *Cell Rep.* 16 (2016) 1942–1953.
- [16] A. Odawara, N. Matsuda, Y. Ishibashi, R. Yokoi, I. Suzuki, Toxicological evaluation of convulsant and anticonvulsant drugs in human induced pluripotent stem cell-derived cortical neuronal networks using an MEA system, *Sci. Rep.* 8 (2018) 10416.
- [17] F. Soldner, J. Laganier, A.W. Cheng, D. Hockemeyer, Q. Gao, R. Alagappan, V. Khurana, L.I. Golbe, R.H. Myers, S. Lindquist, L. Zhang, D. Guschin, L.K. Fong, B.J. Vu, X. Meng, F.D. Urnov, E.J. Rebar, P.D. Gregory, H.S. Zhang, R. Jaenisch, Generation of isogenic pluripotent stem cells differing exclusively at two early onset Parkinson point mutations, *Cell* 146 (2011) 318–331.
- [18] U. Pfisterer, A. Kirkeby, O. Torper, J. Wood, J. Nelander, A. Dufour, A. Bjorklund, O. Lindvall, J. Jakobsson, M. Parmar, Direct conversion of human fibroblasts to dopaminergic neurons, *Proc. Natl. Acad. Sci. U. S. A.* 108 (2011) 10343–10348.